Supporting information

Effects of Cu precursor type on the catalytic activity of Cu/ZrO_2 towards methanol synthesis *via* CO_2 hydrogenation

Shohei Tada,[a] Kazumasa Oshima,[b] Yoshihiro Noda,[b] Ryuji Kikuchi,[a] Minoru Sohmiya,[b] Tetsuo Honma,[c] Shigeo Satokawa [b*]*

a Department of Chemical System Engineering, Graduate School of Engineering, The University of Tokyo, 7-3-1 Hongo, Bunkyo-ku, 113-8656 Tokyo, Japan.

b Department of Materials and Life Science, Faculty of Science and Technology, Seikei University, 3-3-1 Kichijoji-kitamachi, Musashino-shi, Tokyo 180-8633, Japan.

c Japan Synchrotron Radiation Research Institute, Sayo-cho, Sayo-gun, Hyogo 679-5198, Japan.

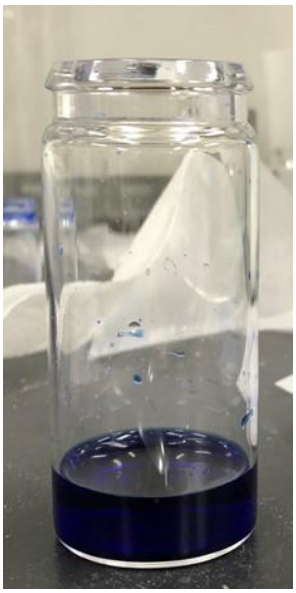

Figure S1 Photograph of copper ammine complex solution.

Section S1 Validation of our experimental condition for N_2O titration

In our previous work, the experimental condition of N_2O titration for Cu-based catalysts were examined using a series of Cu/SiO_2 catalysts [1].

Prior to the examination, H_2 chemisorption for the catalysts was investigated at 25 °C *via* experiments and calculation. We confirmed that H_2 molecules adsorb on the surface of Cu^0 nanoparticles. The maximum H_2 uptake was 0.46 H_2 molecules per Cu surface atoms. The value (0.46) was slightly higher than the stoichiometry of H_2 to Cu (Cu + 0.5 H_2 = Cu-H).

When the N_2O titration was carried out at 90 °C, the amount of decomposed N_2O was almost the same to the H_2 uptake. The experiments clarified that the stoichiometry of N_2O to Cu was 0.5 mol_{N2O} mol_{Cu}^{-1}. The stoichiometry (0.5 mol_{N2O} mol_{Cu}^{-1}) is also expected from the equation of N_2O titration (Cu + 0.5 N_2O = Cu_2O + 0.5 N_2). X-ray absorption spectroscopy measurements showed that the N_2O-treated Cu/SiO_2 catalysts possessed Cu-O scattering path with the distance = 1.82 Å which was similar to that of Cu_2O (1.85 Å) and different from that of CuO (1.96 Å). In consequence, the N_2O titration at 90 °C oxidizes the exposed Cu^0 surface to Cu^+, not the Cu^0 bulk.

Here, we explained the detection way of N_2 and N_2O not using any column. **Figure S2** shows the typical N_2O titration sequence. A thermal conductivity detector was used to measure the gas composition of N_2 and N_2O in a He stream (a carrier gas). In the figure, twenty peaks are observed. The peak size of N_2 must be smaller than that of N_2O due to the thermal conductivity difference: thermal conductivities of N_2, N_2O, and He (a carrier gas) at STP are 0.026, 0.017, and 0.149 W mK^{-1}, respectively [2]. For the first four peaks, their area was *ca.* 55000 count sec and their height was *ca.* 4700 count. The peaks are attributed to N_2 decomposed from N_2O. For the last six peaks, their area was *ca.* 65000 count sec and their height was *ca.* 5500 count. The peaks are attributed to N_2O which was not decomposed on the Cu-based catalysts. In addition, the other peaks are attributed to the mixture gas of N_2 and N_2O. Our previous work [1] also used this detection way and came up with the conclusion described in the previous paragraph.

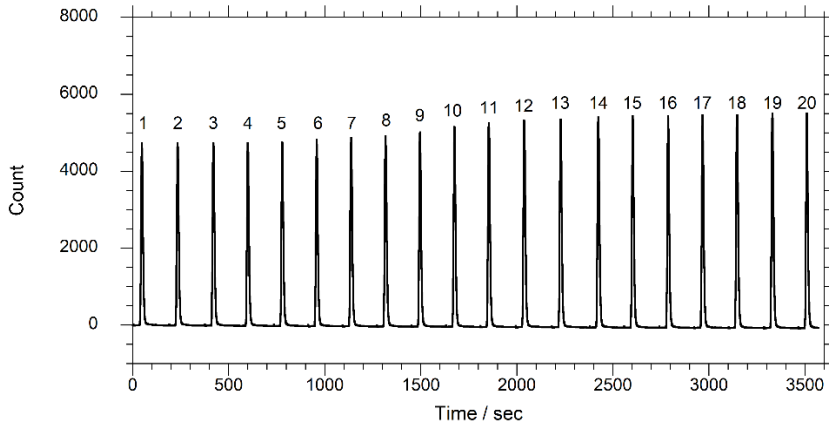

Figure S2 N_2O titration sequence for **NIT-500** at 90 °C. Carrier gas: He.

Table S1 Height and area of peaks in **Figure S1** and N_2/N_2O composition.

No.	Peak height / count	Peak area / count sec	Composition calculated from peak areas / %	
			N_2	N_2O
1	4728	54940	100	0
2	4723	54978	100	0
3	4726	54895	100	0
4	4726	54865	100	0
5	4762	56449	86	14
6	4811	57603	74	26
7	4870	57857	71	29
8	4943	57976	70	30
9	5031	59682	53	47
10	5155	62483	25	75
11	5258	63604	14	86
12	5326	63683	13	87
13	5371	62656	23	77
14	5404	64792	2	98
15	5436	65002	0	100
16	5452	65221	0	100
17	5474	65352	0	100
18	5485	65821	0	100
19	5495	65156	0	100
20	5504	66061	0	100

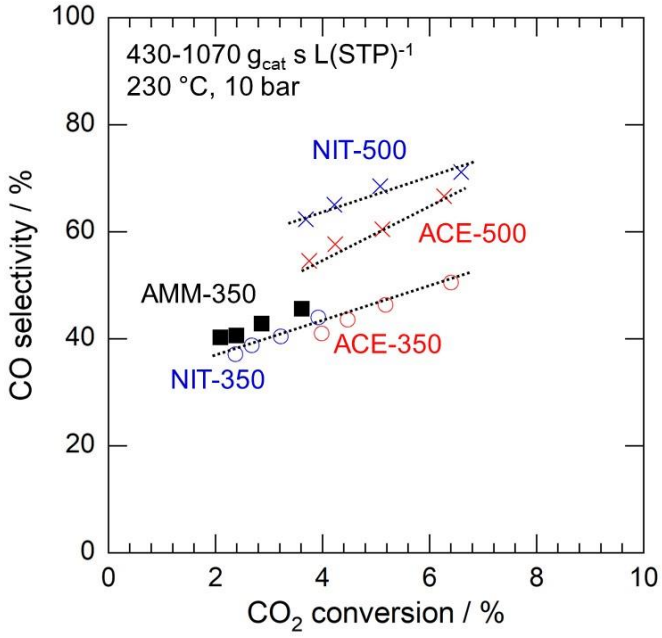

Figure S3 CO selectivity at different CO_2 conversions for **NIT-*T*** and **ACE-*T*** samples.

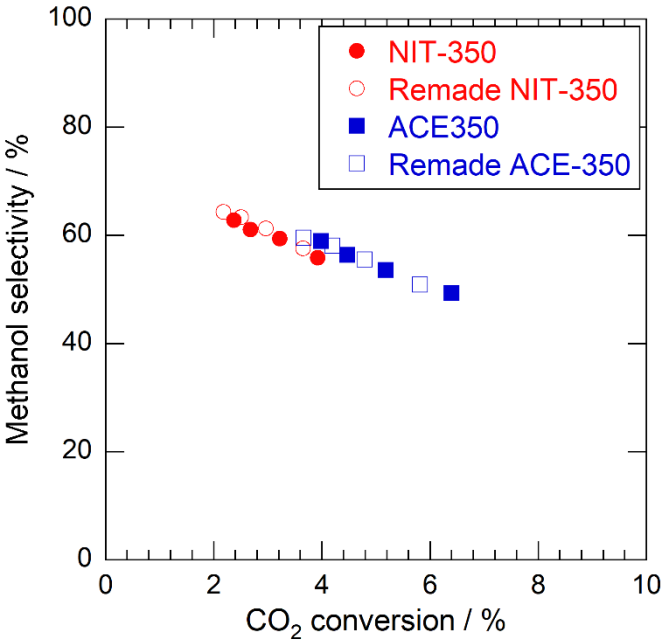

Figure S4 Methanol selectivity at different CO_2 conversion for **NIT-350**, remade **NIT-350**, **ACE-350**, and remade **ACE-350**.

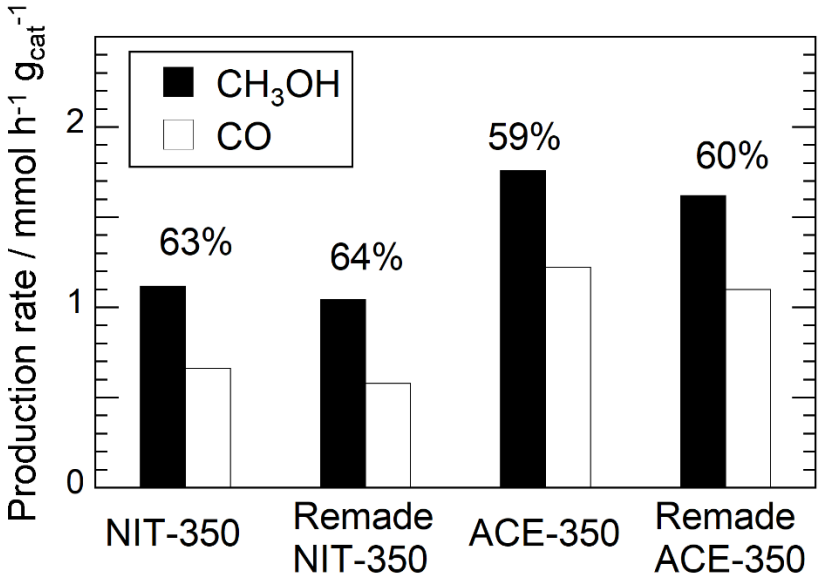

Figure S5 Methanol and CO production rates for **NIT-350**, remade **NIT-350**, **ACE-350**, and remade **ACE-350** when the contact time was 430 g_{cat} s $L(STP)^{-1}$. The values above the bars indicate their selectivity towards methanol.

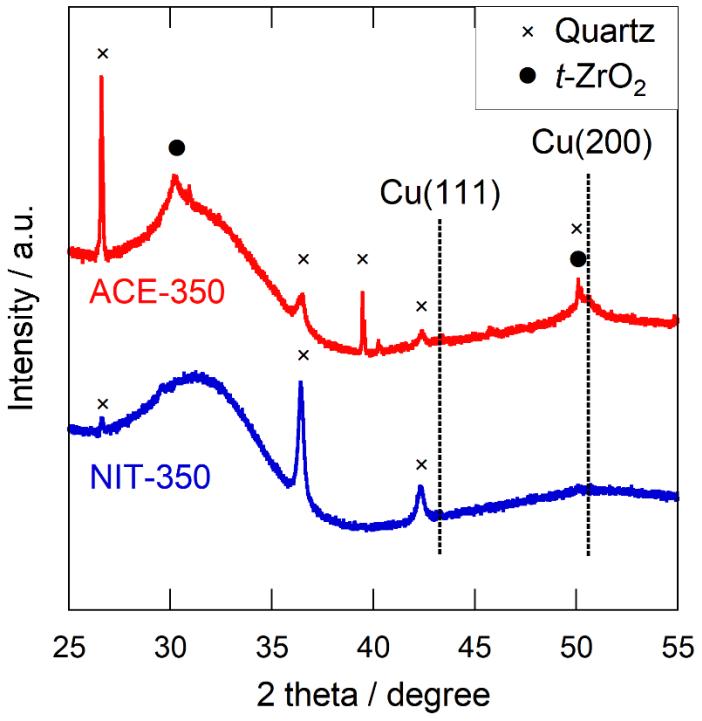

Figure S6 PXRD patterns for spent **ACE-350** and **NIT-350**. Although the quartz sand was removed as much as possible from the spent catalysts, it remained a little and was detected by PXRD.

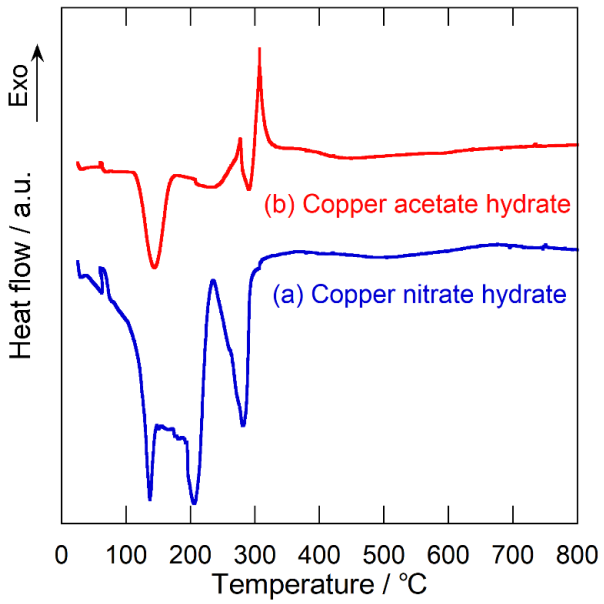

Figure S7 DTA curves for (a) copper nitrate hydrate and (b) copper acetate hydrate. Heating rate: 10 °C min^{-1}.

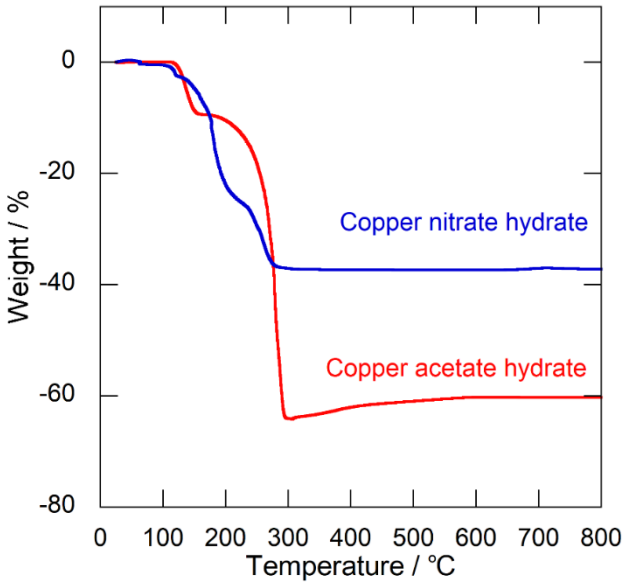

Figure S8 TG curves of copper nitrate hydrate and copper acetate hydrate. For copper acetate hydrate, the sample gains weight with increasing calcination temperature starting from 300 °C. Heating rate: 10 °C min^{-1}.

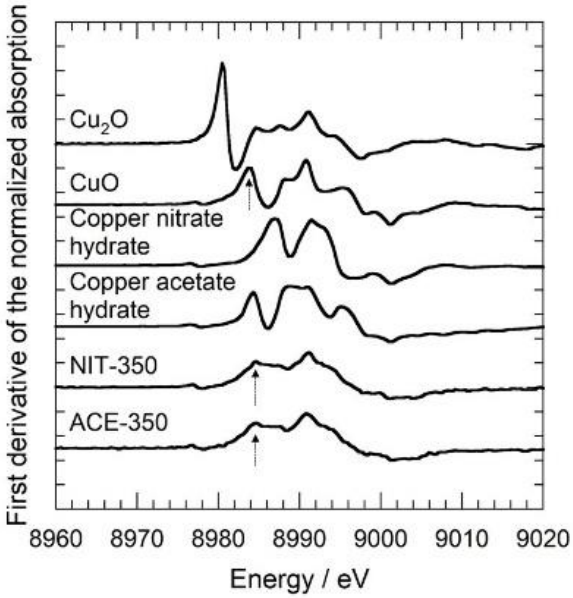

Figure S9 First derivative XANES spectra of **NIT-350**, **ACE-350**, Cu_2O, CuO, copper nitrate hydrate, and copper acetate hydrate. These spectra were obtained at room temperature. The spectra of CuO, **NIT-350**, and **ACE-350** possessed a peak at 8984 eV corresponding to the 1s → 4pπ transition.

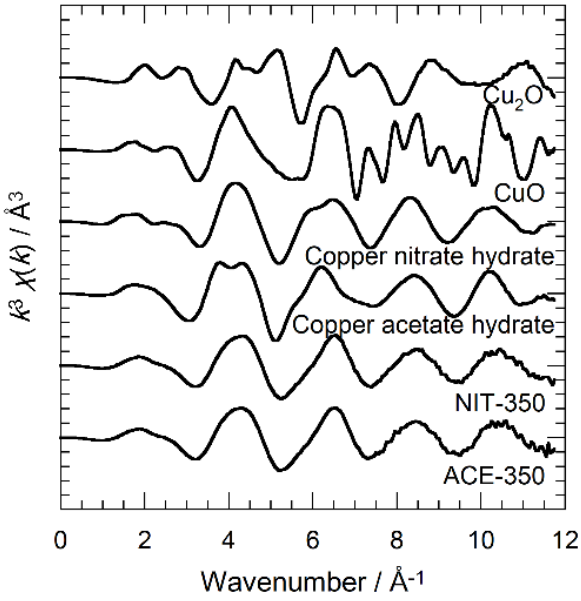

Figure S10 k^3-weighted EXAFS oscillations of **NIT-350**, **ACE-350**, Cu_2O, CuO, copper nitrate hydrate, and copper acetate hydrate measured at room temperature near the Cu K-edge.

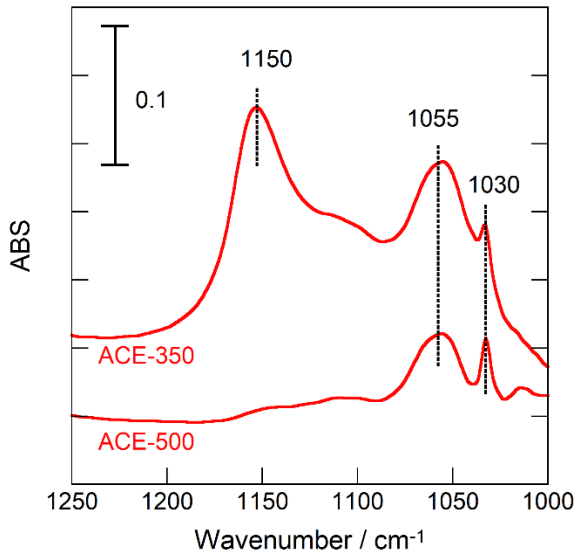

Figure S11 FTIR spectra of methoxy species on ACE-350 and ACE-500.

Methanol vapor sorption on **ACE-350** and **ACE-500** was examined by *in-situ* Fourier transform infrared spectroscopy (*in-situ* FTIR) measurements. The windows of the FTIR cell was high purity CaF_2. The cell was put in a JASCO FT/IR 4600 instrument with a mercury-cadmium-telluride (MCT) detector. The catalyst powder was mixed with KBr (Wako). The weight ratio of the catalyst to KBr was 0.2. The obtained mixture (*ca*. 9 mg_{cat} cm^{-2}) were pressed into a thin self-supporting disk and set in the cell, heated at 330 °C for 30 min under vacuum, and cooled down to 205 °C under vacuum. Then, background spectra were collected at 205 °C. The samples were exposed to methanol vapor (10 kPa) for 5 min at 205 °C. Afterward, the methanol vapor was evacuated for 5 min at 205 °C. Typically, 20 scans were collected for 1 spectrum, and the results were presented as absorbance spectra.

In **Figure S11**, three peaks are observed at 1150, 1055, and 1030 cm^{-1}. According to the reports [3-4], the peak at 1150 cm^{-1} is attributed to on-top methoxy species on Zr^{4+}. The peaks at 1055 cm^{-1} and 1030 cm^{-1} are related to doubly bridging methoxy species on Zr^{4+}. On **ACE-500**, doubly bridging methoxy species were only observed, indicating that most of the surface methoxy species was strongly bounded on ZrO_2. On **ACE-350**, on the other hand, one-top and doubly bridging methoxy species are detected by FTIR. Assuming that a peak area is proportional to the population of the corresponding species, the on-top methoxy species is greater than the doubly bridging methoxy species. Therefore, methoxy species on **ACE-350** adsorbed more weakly on ZrO_2 than that on **ACE-500**.

References

1. Larmier, K.; Tada, S.; Comas-Vives, A.; Coperet, C. Surface Sites in Cu-Nanoparticles: Chemical Reactivity or Microscopy? *J. Phys. Chem. Lett.* **2016**, *7*, 3259-3263.
2. Naterer, G. F., *Advanced Heat Transfer*. Second ed.; CRC Press: Florida, **2018**.
3. Gennari, F. C.; Neyertz, C.; Meyer, G.; Montini, T.; Fornasiero, P. Hydrogen adsorption kinetics on $Pd/Ce_{0.8}Zr_{0.2}O_2$. *Phys. Chem. Chem. Phys.* **2006**, *8*, 2385-2395.
4. Daturi, M.; Binet, C.; Lavalley, J. C.; Galtayries, A.; Sporken, R. Surface investigation on $Ce_xZr_{1-x}O_2$ compounds. *Phys. Chem. Chem. Phys.* **1999**, *1*, 5717-5724.